

Integrating Deformable Trailing Edge Geometry in Modern Mega-Watt Wind Turbine Controllers

Peter B. Andersen Ph.D. student Risø-DTU peter.bioern.andersen@risoe.dk
 Lars C. Henriksen Ph.D. student Risø-DTU lars.christian.henriksen@risoe.dk
 Mac Gaunaa Senior Scientist Risø-DTU mac.gaunaa@risoe.dk
 Christian Bak Senior Scientist Risø-DTU christian.bak@risoe.dk
 Thomas Buhl Senior Scientist Risø-DTU thomas.buhl@risoe.dk

Abstract:

The present work contains a Deformable Trailing Edge Geometry (DTEG) controller algorithm, which is integrated in a numerically simulated modern variable-speed pitch-regulated MegaWatt (MW) wind turbine. Pitot-tubes are mounted on the leading edge of the blades to determine the aerodynamic forces locally on the blade that serves as input for the DTEG. Recent works have shown that the fatigue load reduction by the use of DTEG may be greater than for traditional pitch control methods. By enabling the trailing edge to move independently and quickly along the radial position of the blade, local fluctuations in the aerodynamic forces can be compensated by deformation of the airfoil flap. The aim of this paper is to investigate key parameters like power output, equivalent blade root moment, tower root moments and 10-minute ultimate loads when integrating the DTEG actuators with a conventional wind turbine controller and test it under various turbulent wind conditions. A fatigue reduction of 33% in the tower root moment was obtained for 7 and 18m/s for the 5MW Upwind reference wind turbine from the using pitot-tube sensors mounted on the blades. Furthermore, a reduction of 16% in the tower ultimate root moment over a 10 minute series was seen at 18m/s. The fatigue in the flapwise blade root moment was decreased 48% using an 18m/s averaged wind. Depending on mean wind speeds and choice of control parameters the mean power can also be regulated; an increased mean power production of 1.5% was seen.

Keywords: wind turbine control, deformable trailing edge geometry, pitot tube inflow measurement.

1. Introduction

The traditional variable-speed turbine makes it possible to control the load torque at the generator thus keeping the global axial induction close to

optimum for a wider range of wind speeds by varying the rotational speed of the rotor. Once rated rotational speed is reached the controller will keep the rotation constant. For high wind speeds typically between 11-25m/s, the pitch and generator torque will keep the power constant. Pitch-regulating a blade means changing the Angle Of Attack (AOA) throughout the spanwise cross-sections and with the exception of structural deformations like torsional twist all sections should react collectively to the pitching motion.

The work presented in this paper will extend the traditional variable-speed pitch-regulated control to include Deformable Trailing Edge Geometry (DTEG) in a pitch-flap-regulated control algorithm using a series of Pitot-Tube (PT) sensors mounted on the blade along with Strain-Gauges (SG) mounted near the blade root as input for the control.

Adding a flap at the trailing edge to a wing is a well known method for changing the aerodynamic pressure distribution around the wing. At Risø National Laboratory, Denmark, a continuous research of using a DTEG for reducing load fluctuations on wind turbines have been carried out [1,3-8,16]. A number of DTEG configurations have previously been tested by Risø. For the purpose of this paper the DTEG will be characterized by a smooth and continuous gradient from the non-deformable part of the airfoil to the deformable part. This type of DTEG was chosen in Risø's previous work because flow separation and thereby corresponding noise and drag was reduced, compared to the rigid flap. Now the DTEG is implemented in a turbine control algorithm. The effect of Trailing Edge (TE) eddy shedding is included in the control algorithm.

The turbine is based on the 5MW Upwind reference turbine [11]. The blade has a length of 63.0m. The 331 tones tower has a length of 79.6 m. Shaft and nacelle has a total weight of 240 tonnes. The Delft DU profile series is used on the blade. The blades have a max chord of 4.7m at the radial position 15.9m from

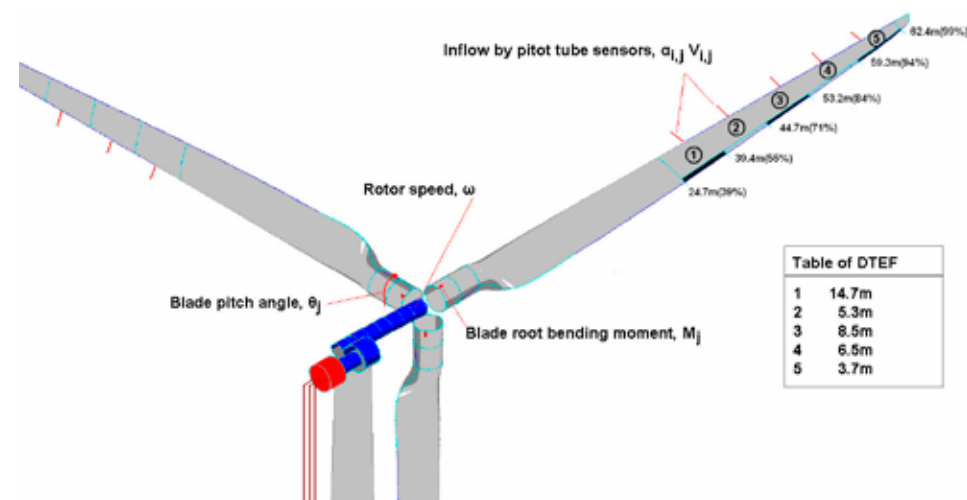


Figure 1: Five DTEG's (marked 1-5) with corresponding PT used to feed the input for the control. In total 60% of the blade radial length will be flappable.

the blade root (overall rotor solidity is 5.4%). The present control will be implemented and tested in the aero-servo-elastic code HAWC2 [2]. The program comprises a multi body model based on Timoshenko beam elements, where the turbine is divided into substructures like tower, nacelle and rotor blades. Each substructure has its own coordinate system allowing for rotations of the substructures. There are six Degrees Of Freedom (DOF) for each element node. Aerodynamic torque, thrust and other loads are dynamically calculated in HAWC2 using an unsteady Blade Element Momentum (BEM) model approach. The local aerodynamic load is calculated at the blade section using 2D lift, drag and moment profile coefficients, having been corrected for 3D and rotational effects using the Viterna method [15] for 0-90 degrees AOA. The dynamic stall model by Andersen et al. [1] for the DTEG along with a dynamic inflow [12] model and tip loss found in Wilson and Lissaman [14] is also included in HAWC2. No attempt has been made to simulate the actual electrical properties of the generator or the grid connections. The sum of losses in the gearbox, converter and generator is 5.6% at rated power with a gearing ratio of 97. Parameters like length scales and shear distortion for the turbulence is provided by IEC61400-

1 and will be used at three different mean wind speeds 7.0m/s, 11.4m/s and 18.0m/s with turbulence intensity at 14-18%. Ten minute turbulence time series based on Gaussian homogenous coherence cross-spectral models for the Shimozuka algorithms implemented in the Mann turbulence model is used. In all cases no yaw misalignment is used. Wind shear with a power coefficient of 0.14 seen at Havsøre [17] is part of the simulation along with a potential tower shadow model.

Previous studies by Andersen et al [7] provided a detailed study of optimal placement, length and number of flaps for a blade; these studies were performed for constant rotational rotor speed. For the purpose of this study, five DTEG per blade are located as shown in Figure 1. The fifteen DTEG actuators are individually controlled and operated inside a +/- 8 degree interval with no constraints on deflection rate which experiments showed viable for piezo-electric actuators. The pitch and generator servo is modeled as a first order system with time constants 0.2 and 0.1 seconds respectively. The controller cuts off pitch rates greater than 8 deg/s.

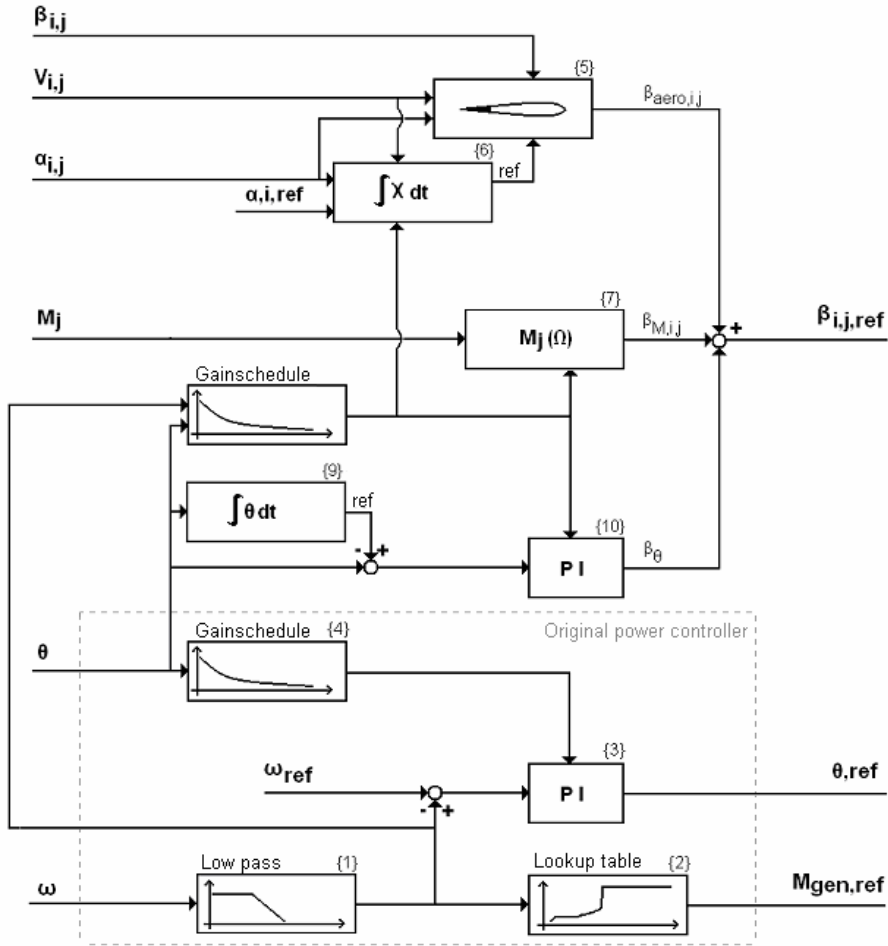


Figure 2: Control diagram of regulator. Input is measured rotational rotor speed, pitot tube mounted on blades, blade root moment and output is reference moment for the generator a reference collective pitch angle and flap deflection angles. Index "i" marks the DTEG number located on blade number "j".

2. Controller design

The traditional controller is taken from the work of Hansen et al. [13], where the controller is build around a PI-regulator which actuates the blade pitch using the rotational speed of the High Speed Shaft (HSS) as input. The DTEG has been added to this original design using a series of PT mounted on the blades and Strain Gauges (SG) mounted near the blade root. Figure 2 illustrates a full controller diagram. It is important to avoid high frequency drive train vibration especially the free-free drive train vibration. As it can be seen in Figure 2 a special low pass filter, control block {1}, has been added with a cutoff at -3dB approximately a quarter of the edgewise eigenfrequency as specified by Jonkman [11]. The generator torque, control block {2}, is given as a function of the HSS, cut-in at 70.2rad/s, starting variable speed region at 91.2rad/s ending at 121.7rad/s, where the generator torque is given by a simple K-omega square model, a steeper slope of 3935Nm/(rad/s) yield generator torque until rated power, at which point the torque is given by power over rotational speed of the HSS. To control the aerodynamic power a series of PI-regulators are added to adjust the reference pitch and the DTEG deflections. Once the HSS exceeds 122.9rad/s the pitch actuator starts handling low frequency changes in the aerodynamic fluctuations, whereas, the DTEG controllers alleviates high frequency aerodynamic fluctuations and non aerodynamic fluctuations, such as gravitational loads coupled with flapwise root bending moment as well as contributions from inertial and fictitious forces not captured by the PT sensors for all wind speeds. The PI-regulator, control block {3}, has a minimum setting of zero degrees pitch for low wind speeds. Highly pitched blades require smaller changes in pitch angles in order to regulate the power production due to the changed orientation of the lift component relative to the rotor plane. For highly pitched blades, the lift vector is less perpendicular to the rotor plane than a blade which is operating below rated power. A pitch gain scheduling, part of control block {4}, has been included to compensate for the increased pitching effect at high wind speeds. The pitch gain scheduling (ψ) is described in the work of Hansen et al. [13] and can be seen in Equation (1)

$$\psi(\theta) = \frac{1}{1 + \frac{\theta}{KK}} \quad (1)$$

where KK represent the pitch angle (θ) where the derivative of the aerodynamic power, with respect to pitching angle, has increased by a factor of two relative to the derivative at rated pitch.

The DTEG controller reacts to changes in aerodynamics, structural dynamics and pitch motion, by three decoupled contributions to the overall DTEG deflection (β_{ref})

$$\beta_{i,j,ref} = \beta_{aero,i,j} + \beta_{M,i,j} + \beta_{\theta,i,j} \quad (2)$$

where (β_{aero}) marks the DTEG deflection contribution from PT sensors, (β_M) the contribution from the SG sensor mounted near the blade root and (β_{θ}) the contribution from blade pitch. Index "i" marks the section number which has a DTEG located on blade number "j". The pitch handles low frequency aerodynamic changes on rotor scale, whereas, the DTEG handles high frequency fluctuations locally on the blade. The aerodynamic contribution to the DTEG deflection at control block {5} is derived from the traditional BEM model, which simplifies the aerodynamics of a rotor by dividing a blade into a number of 2D cross sections. The lift force for a section is

$$L_{i,j} = \frac{1}{2} \rho c_i V_{i,j}^2 C_{L,i,j} \quad (3)$$

The local AOA is labeled (α). The (C_L) marks the lift coefficient, (V) is the relative wind speed seen by the blade with a local chord (c). Shed vorticity is introduced as

$$C_{L,i,j} = \left[\frac{\partial C_L}{\partial \alpha} \right] (\alpha_{i,j} - \alpha_{a,i,j}) + \left[\frac{\partial C_L}{\partial \beta} \right] \beta_{aero,i,j} \left[1 - \sum_{k=1}^3 A_k \right] + \sum_{k=1}^3 z_{i,j,k} \quad (4)$$

where index "k" separate the two/three shed vorticity state variables (z) with corresponding constants (A_k , b_k). The three wake state variables (z) are given by

$$\frac{\partial z_{i,j,k}}{\partial t} + b_k z_{i,j,k} = A_k b_k \left[\frac{\partial C_L}{\partial \alpha} \right] (\alpha_{i,j} - \alpha_{a,i,j}) + \left[\frac{\partial C_L}{\partial \beta} \right] \beta_{i,j} \quad (5)$$

The constants (A_k) and (b_k) are profile specific and suggested by Jones [9] for a flat plate. The shed vorticity effects in the wake can be included using a number of indicial functions outlined by Von Karman et al [10]. The running averaged reference (χ) shown in control block {6} over a period is given by

$$\chi = \frac{1}{3\tau_{aero}} \int_{t-\tau_{aero}}^t \sum_{j=1}^3 V_{i,j}^2 \left[\frac{\partial C_L}{\partial \alpha} (K_a \alpha_{i,ref} + (1-K_a) \alpha_{i,j} - \alpha_{o,i}) + \frac{\partial C_L}{\partial \beta} \beta_{i,j} \right] dt \quad (6)$$

By changing the aerodynamic time constant, it is possible to determine which aerodynamic frequencies the DTEG will respond to. If the only purpose of the controller is to minimize fatigue for the blade root moment, it is recommended to scale the time constants (τ_{aero}) with the rotational speed of the rotor. Using 2.5 seconds for all wind speeds balances the load reduction for more wind turbine components. However, Figure 3 illustrates the dilemma of choosing between reducing tower root loads or blade root loads. The suggested controller presented in the paper does not seem to provide an optimal reduction for both blade root and tower root moments at high wind speed. For lower wind speeds this dilemma is not as pronounced. The power optimization coefficient (K_a) is used for targeting specific AOA in the variable speed region seeking thrust levels which yield optimal axial inductions at maximum gliding numbers if the planform of the blade is well designed. As default K_a was zero, a single simulation was made using $K_a=1$ for the variable speed region and $K_a=0$ for higher wind speeds. For illustration see Table 1 and Figure 6. The

aerodynamic contribution to the DTEG deflection angle for a movable cross section is found by rewriting Equations (3-6)

$$\beta_{aero,i,j} \leftarrow \frac{1}{\frac{\partial C_L}{\partial \beta}} \left\{ \frac{\chi}{V_{i,j}^2} - \sum_{k=1}^3 z_{i,j,k} - \frac{\partial C_L}{\partial \alpha} (\alpha_{i,j} - \alpha_{o,i}) \right\} \quad (7)$$

Another component in the control loop is the blade root moment (M), which is expected to be measured using a series of SG sensors mounted near the root of the blade. Based on the assumption that some aerodynamic excitation on one blade will be seen later on the following blade with a 120 degree phase shift in azimuthal angle (Ω), the root moment measurement is used in the control in a feed-forward manner.

$$\Delta M_j(\Omega) = M_j(\Omega) - \langle M_j \rangle = \sum_{i=1}^{n_p} \Delta M_{i,j}^* \quad (8)$$

where (n_p) mark the number of DTEG's mounted on the blade and (Kp_i) mark the DTEG scheduling factor see Figure 4. These factors are found calling HAWC2 using a simplex algorithm style. The blade root moment response to a DTEG step change for each of the five DTEG's is shown in Figure 10 along with the fitted coefficients (A_m) and (b_m) for the indicial formulation used in the control.

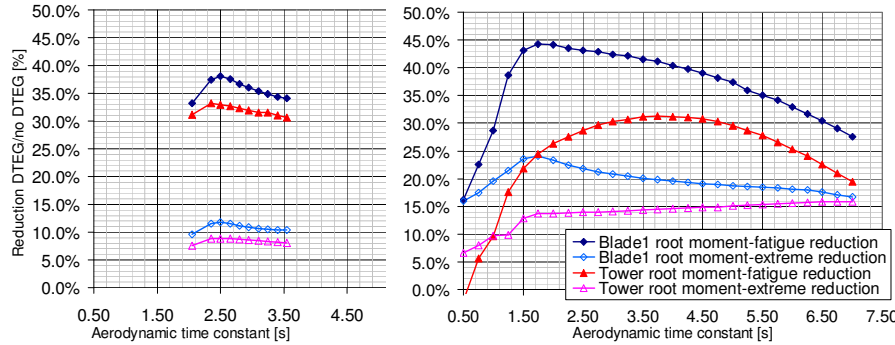


Figure 3: Blade 1 root and tower root load reductions for a 10 minute turbulent (right) 18m/s average and (left) 7m/s average wind series varying the aerodynamic time constant.

$$\Delta M_{i,j}^* = \left(1 - \sum_{m=1}^4 A_m \right) \frac{\partial M}{\partial \beta} \Big|_i Kp_i \beta_{i,j} + \sum_{m=1}^4 z_{i,j,m} \quad (9)$$

where the state variable (z_m) keeps track of the dynamic response in the blade root moment when using one of the five DTEG's.

$$\frac{\partial z_{i,j,m}}{\partial t} + b_m z_{i,j,m} = A_m b_m \frac{\partial M}{\partial \beta} \Big|_i Kp_i \beta_{i,j} \quad (10)$$

The contribution from the SG sensor, which is marked as control block {7} in Figure 2, comprises Equation (11). The phase angle (Φ) is used to help approximate the time lag (see Figure 10) in root moment response from a DTEG step change.

$$\beta_{M,i,j} \leftarrow \frac{\Delta M_{i,j}(\Omega - \phi) - \sum_{m=1}^4 z_{i,j,m}}{\left(1 - \sum_{m=1}^4 A_m \right) \frac{\partial M}{\partial \beta} \Big|_i} Kp_i \quad (11)$$

Using a running average pitch motion, control block {9} in Figure 2, the blade pitch motion is taken into account which is important in order to avoid that the DTEG counter-reacts the pitching motion, putting yet more strain on the pitch servo. The contribution from the pitching motion to the DTEG controller is provided in Equation (12)

$$\beta_\theta \leftarrow K_{p,\theta} \left(\theta - \frac{1}{\tau_\theta} \int_{t-\tau_\theta}^t \theta dt \right) \quad (12)$$

where the PI regulator, control block {10} in Figure 2,

comprises a proportional gain feedback loop with the integral gain imbedded using a time constant (τ_θ) of 4.0 seconds.

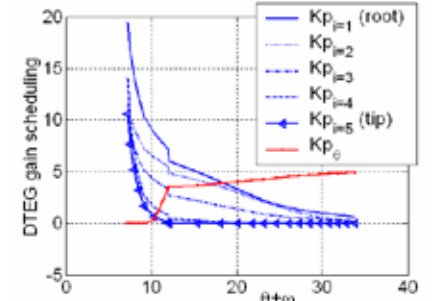


Figure 4: The DTEG gain scheduling is based on both rotational speed of rotor and the pitch setting.

3. Results

A series of step responses have been used to evaluate the behavior of the controller. The wind speed is increased by 1m/s at intervals of 40s. There is no turbulence, wind shear nor tower shadow only the tilt angle of 5 degrees contributes to varying aerodynamic inflow during a rotor revolution.

In Figure 5 the power response at $t=320s$ yields less overshoot using the DTEG controller, when stepping from 10-11m/s in free wind. Notice how the DTEG absorbs the 1P fluctuations partially due to the tilt of the nacelle. The 7m/s average turbulent wind case is

	10 min. turb. series of	<7m/s> $K_a=0$ (Figure 6)	<7m/s> $K_a=1$ (Figure 6)	<11m/s> (Figure 8)	<18m/s> (Figure 9)
Reduction in					
Max blade1, flapwise root moment		11.8%	6.5%	16.0%	24.0%
Max tower, flowwise root moment		8.8%	2.6%	6.5%	15.9%
Blade1, equivalent flapwise root moment		38.1%	36.2%	45.5%	47.9%
Tower, equivalent flowwise root moment		33.2%	31.9%	20.8%	33.3%
Pitch rate, standard deviation		n/a	n/a	10.9%	19.0%
Mean power prod. (-loss) without DTEG		1375KW	1375KW	4694KW	5291KW
Mean power prod. (-loss) with DTEG		1364KW	1395KW	4682KW	5300KW
Percent change in power production		-0.8%	+1.5%	-0.2%	+0.2%

Table1: compiled results based on the 10 minute series.

shown in Figure 6. The duration of the simulation is the default 10 minute the controller operates in the variable speed region where pitching activity is close to zero. Besides showing the original power controller in Figure 6, two DTEG controller settings are tested. The first setting forces the DTEG to target a moving reference lift ($K_{\alpha}=0$), which is the default; the other setting enables the controller to target an optimal thrust or axial induction at a designed AOA which should ensure an optimal aerodynamic power conversion. Even though there is an increased power production at the expense of a higher thrust shown in both Table 1 and Figure 6 the overall load reduction potential is still favorable when using DTEG's compared to the original pitch regulated power controller. A decrease in load reductions is seen for $K_{\alpha}=1$ compared to the $K_{\alpha}=0$ case indicating the tradeoff between power and load optimization. Figure 7 is a power spectral plot for the blade root moment; the plot reveals that a wide range of frequencies have been damped out. In Figure 8 the averaged turbulent wind speed is 11m/s, in this region the turbine experiences the highest loads e.g. in thrust. Both blade1 and tower root moment seems smoother and pitching activity starts later and stops earlier compared to the original controller. Once pitching activities starts the rate of pitching is comparable or perhaps even slightly increased locally compared to the original controller, see $t=585-595s$ in Figure 8. The result of the highest wind speeds are shown in Figure 9. Loads are smoother and power production is slightly higher using the DTEG controller. There seems to be a 0.6Hz oscillation for the pitch rate signal for both controllers at $t=235-240s$ in Figure 9.

For a better comparison the results are compiled in Table 1. There is a general decreased pitch activity when using DTEG, especially for high wind speeds. The power production can vary between -0.8 to 1.5 percent depending on wind speed and choice of K_{α} setting compared to the traditional controller. A fatigue reduction of 33% in the tower root moment is obtained for 7 and 18m/s, a reduction of 16% in the tower ultimate root moment at 18m/s is seen. The fatigue in the flapwise blade root moment is decreased 48% for high wind speeds. Although the load reductions are higher (in percentage) at 18m/s, the reduction potential at 11m/s should have the highest regards as the blades is stressed the most in this control region under normal working conditions. Depending on mean wind speeds and choice of control parameter the power can be regulated. An increase in mean power production of 1.5% is seen.

In all this paper suggests an extended power controller using a series of DTEG. For the variable speed region, the controller seems to be able to extract more energy from the wind at the expense of an increased mean thrust level. It is difficult to determine how much this effect is due to a poorly tuned reference controller and how much is due to compensation of local effects like blade torsional deflection. There seems to be a 0.6Hz oscillation in both controllers which indicates that the interaction between DTEG and pitch controller could be improved. The suggested controller can decrease the ultimate blade root load up to 24% for high wind speeds and 16% at the highest thrust levels. For the 10-minute ultimate tower root moment a similar pattern is seen although somewhat lower reductions 15.9% and 6.5% are obtained. The rate of pitch is decreased by 10-19% in standard deviation. For all wind speeds the new controller shows significant fatigue reductions for blade and tower root moments well above 30-40%.

4. Conclusion

A new wind turbine controller algorithm which, in addition to traditional pitch control, includes local control by Deformable Trailing Edge Geometries (DTEG) has been investigated. The controller is designed for the 5MW Upwind reference turbine and tested in wind speeds ranging from cut-in to cut-out i.e. 4-25m/s

Significant load reduction is obtained; overall pitch activity is decreased with some local unwanted fluctuations which may require further investigation. A fatigue reduction of 33% in the tower root moment is seen for 7 and 18m/s. The fatigue loads in the flapwise blade root moment is decreased 48% and the tower 10 minute ultimate root moment is decreased 16% at 18m/s average turbulent wind.

The power yield is not affected in a significant way for the constant tip-speed control regime; in fact, an increase of 1.5% in power output was obtained for given control parameters.

The complexity in the suggested controller design model is believed to balance the significant load reductions obtained and presented in this work.

References

- [1] Andersen P.B., Gaunaa M., Bak C., Hansen M.H., "A Dynamic Stall Model for Airfoils with Deformable Trailing Edges", Journal of Physics 5, 2007 and oral presentation on "2nd EWEA,EAWE The Science of making Torque from Wind conference at DTU, 28-31 August 2007".
- [2] Larsen T.J., Hansen A.M. "Influence of Blade Pitch Loads by Large Blade Deflections and Pitch Actuator Dynamics Using the New Aeroelastic Code HAWC2", paper and oral presentation at EWEC 2006, Athens, 2006.
- [3] Basualdo, S., "Load alleviation on wind turbine blades using variable airfoil geometry", Wind Engineering, vol. 29, no. 2, 2005
- [4] Trolborg, N., "Computational study of the Risø-B1-18 airfoil with a hinged flap providing variable trailing edge geometry", Wind Engineering, vol. 29, no. 2, 2005
- [5] Buhl, T.; Gaunaa, M.; Bak, C.; "Potential Load Reduction Using Airfoils with Variable Trailing Edge Geometry"; Journal of Solar Energy Engineering; November 2005, Vol. 127, p. 503-516
- [6] Gaunaa, M., "Unsteady 2D Potential-flow Forces on a Thin Variable Geometry Airfoil Undergoing Arbitrary Motion", Risø-R-1478, Risø, Denmark, June 2004
- [7] Andersen, P.B.; Gaunaa, M.; Bak, C.; Buhl, T., "Load alleviation on wind turbine blades using variable airfoil geometry." In: Proceedings (online). 2006 European Wind Energy Conference and Exhibition, Athens (GR), 27 Feb -2 Mar 2006. (European Wind Energy Association, Brussels, 2006) 8 p
- [8] Abdallah, I.; "Advanced Load Alleviation for Wind Turbines using Adaptive Trailing Edge Geometry: Sensing Techniques." M.Sc Thesis Project; July 13, 2006, Technical University of Denmark, Department of Mechanical Engineering, Section of Fluid Mechanics
- [9] Jones,R.T.,"The Unsteady lift of a Wing of finite Aspect-ratio",Tech.Rep.681, NACA rep, 1940
- [10] Von Karman, Th. & Sears, W.R., "Airfoil Theory for Non-Uniform Motion.", Journal of the Aerodynamical Science. 5(10) 1938. p.379-390
- [11] <http://wind.nrel.gov/public/ijonkman/NRELOffshrBslime5MW/NRELOffshrBslime5MW.pdf>
- [12] Sørensen, N.N., Madsen, H.A., "Modelling of transient wind turbine loads during pitch motion." In: Proceedings (online). 2006 European Wind Energy Conference and Exhibition, Athens (GR), 27 Feb -2 Mar 2006.
- [13] Hansen, M.H., Hansen A., Larsen T.J., Øye S., Sørensen P. and Fuglesang P. "Control design for a pitch-regulated, variable speed wind turbine", Risø-R Report, Risø-DTU National Laboratory, Risø-R-1500(EN). Januar 2005.
- [14] Wilson, R.E. and Lissaman, P.B.S. "Applied Aerodynamics of wind power machines", Oregon State University, May 1974.
- [15] Snel, H. (ECN), Houwink, R. (NLR), and Bosschers, J. (NLR) "Sectional prediction of lift coefficients on rotating wind turbine blades in stall". ECN-C-93-052, Petten, December 1994.
- [16] Bak, C.; Gaunaa, M.; Andersen, P.B.; Buhl, T.; Hansen, P.; Clemmensen, K.; Møller, R., "Wind tunnel test on wind turbine airfoil with adaptive trailing edge geometry." In: [Technical papers] presented at the 42. AIAA aerospace sciences meeting and exhibit. 45. AIAA aerospace sciences meeting and exhibit, Reno, NV (US), 8-11 Jan 2007. (American Institute of Aeronautics and Astronautics, Reston, VA, 2007) (AIAA-2007-1016)
- [17] Madsen, H.A., Mikkelsen R., Sørensen N.N., Hansen O.L.M., Øye S., Johansen J., "Influence of wind shear on rotor aerodynamics, power and loads", In: Research in Aeroelasticity EFP-2006. Risø-R Report, Risø-DTU National Laboratory. July 2006. Risø-R-1611(EN)

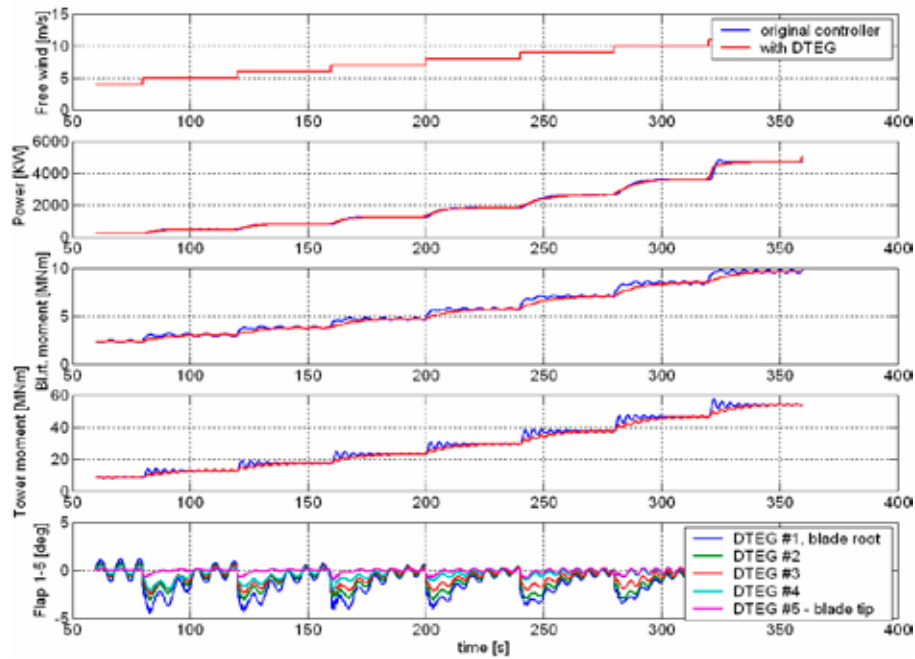


Figure 5: (from top down) free wind at hub height, electrical power, flapwise blade root moment, tower root moment in flowwise direction, DTEG deflection angles.

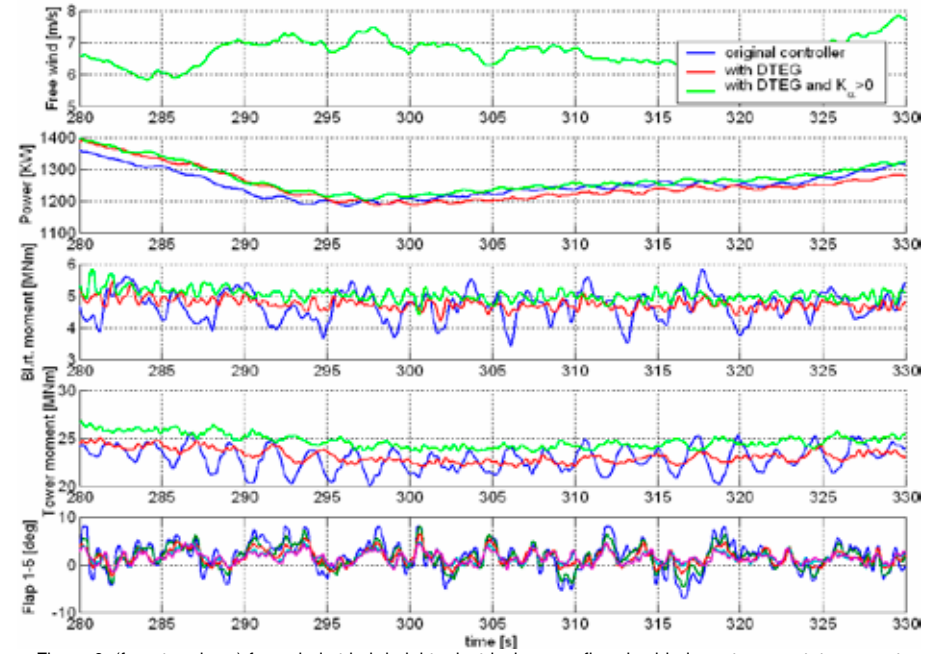


Figure 6: (from top down) free wind at hub height, electrical power, flapwise blade root moment, tower root moment in flowwise direction, DTEG deflection angles.

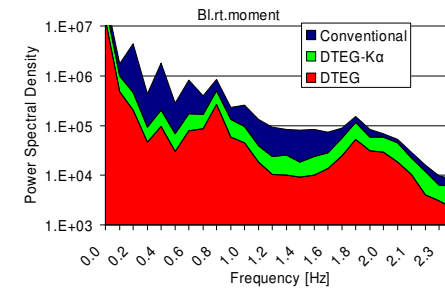


Figure 7: Power Spectral Density (PSD) of blade 1 flapwise root moment; based on a 10-minute series.

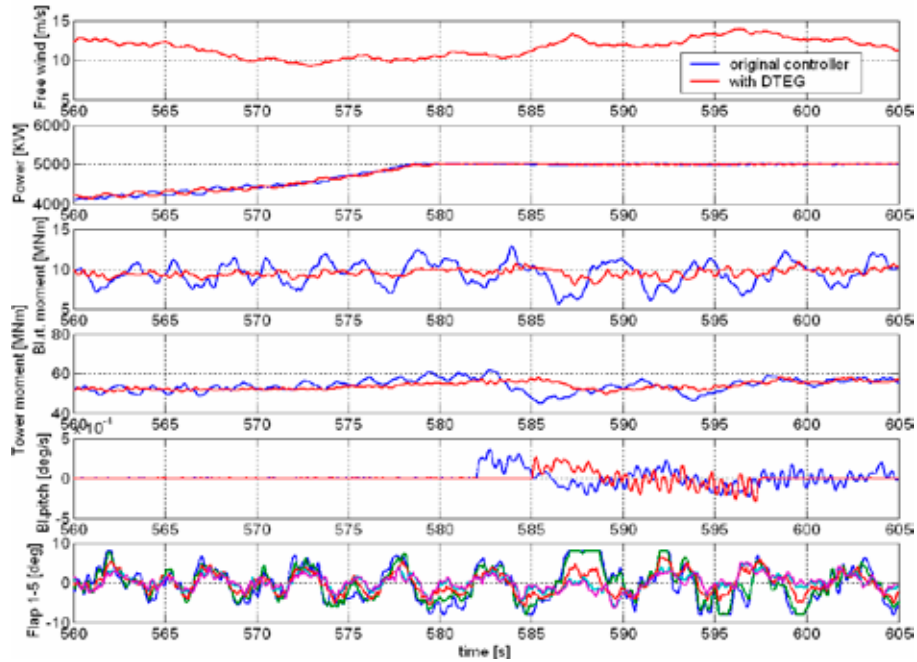


Figure 8: (from top down) free wind at hub height, electrical power, flapwise blade root moment, tower root moment in flowwise direction, collective pitch speed, DTEG deflection angles.

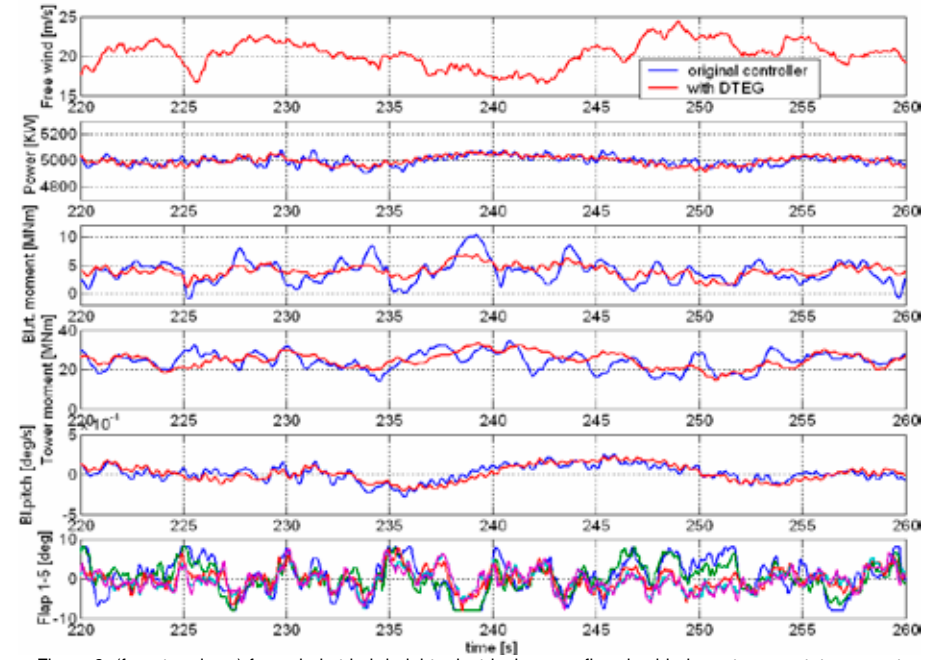


Figure 9: (from top down) free wind at hub height, electrical power, flapwise blade root moment, tower root moment in flowwise direction, collective pitch speed, DTEG deflection angles.

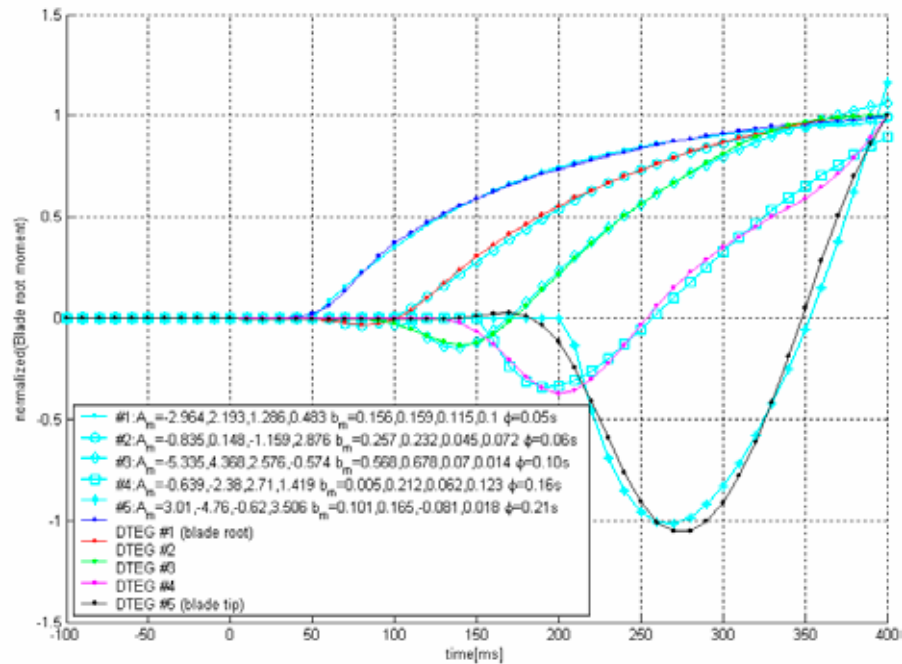


Figure 10: Five responses in blade root moments for blade 1 all based on HAWC2 simulations using the 5MW reference turbine used in the Upwind project. The normalized blade root moment response to a DTEG step change from 0 to 8 degree positive deflection. Responses for each of the five DTEG's is shown along with the fitted coefficients (A_m) and (b_m) used in the indicial formulation. The phase lag (ϕ) is used to help approximate the time lag in response.